MS. MEGAN LEE FEDDERN (Orcid ID : 0000-0002-5863-7229)
DR. ERIC J WARD (Orcid ID : 0000-0002-4359-0296)

Article type : Primary Research Articles

Title: Stable isotope signatures in historic harbor seal bone link food web-assimilated carbon and nitrogen resources to a century of environmental change

Running Title: *(42 of 45 characters with spaces)* Changing food web-assimilated resources

Authors: Megan L. Feddern[1], Gordon W. Holtgrieve[1], Eric J. Ward[2]

1. University of Washington, School of Aquatic and Fishery Sciences, 1122 NE Boat Street, Seattle, WA 98105

2. Conservation Biology Division, Northwest Fisheries Science Center, National Marine Fisheries Service, 2725 Montlake Boulevard East, Seattle, WA 98112

Corresponding Author: Megan L. Feddern, 603-651-6802, mfeddern@uw.edu

Main text: 6737 of 8000 words

Abstract (300 of 300 words)

Anthropogenic climate change will impact nutrient cycles, primary production, and ecosystem structure in the world's oceans, although considerable uncertainty exists regarding the magnitude and spatial variability of these changes. Understanding how regional-scale ocean conditions control nutrient availability and ultimately nutrient assimilation into food webs will inform how marine resources will change in response to climate. To evaluate how ocean conditions influence the assimilation of nitrogen and carbon into coastal marine food webs, we applied a novel dimension reduction analysis to a century of newly acquired molecular isotope data derived from historic harbor seal bone specimens. By measuring bulk $\delta^{13}C$ and $\delta^{15}N$ values of source amino acids of these top predators from 1928-2014, we derive indices of primary

production and nitrogen resources that are assimilated into food webs. We determined coastal food webs responded to climate regimes, coastal upwelling, and freshwater discharge, yet the strength of responses to individual drivers varied across the northeast Pacific. Indices of primary production and nitrogen availability in the Gulf of Alaska were dependent on regional climate indices (i.e., North Pacific Gyre Oscillation) and upwelling. In contrast, the coastal Washington and Salish Sea food webs were associated with local indices of freshwater discharge. For some regions (eastern Bering Sea, northern Gulf of Alaska) food web assimilated production was coupled with nitrogen sources, however other regions demonstrated no production-nitrogen coupling (Salish Sea). Temporal patterns of environmental indices and isotopic data from Washington state varied about the long-term mean with no directional trend. Data from the Gulf of Alaska, however, showed below average harbor seal $\delta^{13}C$ values and above average ocean conditions since 1975, indicating a change in primary production in recent decades. Altogether, these findings demonstrate stable isotope data can provide useful indices of nitrogen resources and phytoplankton dynamics specific to what is assimilated by food webs.

Keywords (8 of 8)

climate change, amino acid, compound-specific stable isotope analysis, northeast Pacific Ocean, harbor seals, primary production, Gulf of Alaska

Introduction

Changing ocean conditions are reshaping the structure and function of marine food webs on regional scales. Ocean temperature (Hoegh-Guldberg and Bruno 2010), oxygen availability (Brietbrg et al. 2018), and climatic regimes such as El Niño Southern Oscillation (ENSO) (Vecchi and Wittenberg 2010) alter nutrient availability and cycling, and thus, the ecological structure of marine systems. Projected global redistribution of nutrients suggests net primary production in the ocean is likely to change both spatially and temporally. Yet, substantial uncertainty remains, with predictions suggesting both increases and decreases in global net primary productivity of up to 20% by 2100 (Bopp et al. 2013; Kwiatkowski et al. 2017, Gregg et al. 2003). An important contributor to this uncertainty is regional variability in phytoplankton response to ocean conditions and how that variability will impact other trophic levels and dependent fisheries (Moore et al. 2018, Brander 2010). Ocean conditions (i.e., sea surface temperature, freshwater discharge, wind, and ice cover) have been associated with abundance and recruitment of many fish species in the Northeast Pacific (Cunningham et al. 2018, Puerta et

al. 2019, Stachura et al. 2014). Nonetheless, these studies rarely include indicators of nutrient availability or primary production linking the ecosystem response to its environment. Understanding how regional and local scale physical drivers control nutrient availability and ultimately nutrient assimilation into food webs will be important for predicting the future availability of marine resources.

A strong empirical understanding of food web response to changing ocean conditions and nutrient constraints requires time series data that span multiple climate regimes to decouple natural variability with long-term anthropogenic changes. Currently, quantitative methods are also limited in their ability to scale primary production trends to ecosystem-level responses (Bonan and Doney 2018). Stable isotope measures of $\delta^{15}N$ ($^{15}N/^{14}N$) of individual amino acids is an emerging tool for reconstructing trends in nitrogen sources from historic specimens (McMahon et al. 2019, Sherwood et. al. 2011, Sherwood et al. 2014, Whitney et al. 2019). The $\delta^{15}N$ signature at the base of the food web is primarily controlled by utilization and the isotopic signatures of different nitrogen sources, particularly urea, nitrate, and ammonium, by primary producers (Graham et al. 2010, Ohkouchi et al. 2017). Measurements of bulk $\delta^{15}N$ values from consumers can be difficult to attribute to changes at the base of the food web because trophic level shifts also effect the isotopic composition of bulk nitrogen (Fry 2006). Amino acid specific $\delta^{15}N$ data addresses this challenge, as amino acids exhibit two distinct patterns in isotopic enrichment: trophic amino acids (i.e., glutamic acid, alanine, proline) become enriched in ^{15}N with each trophic transfer and source amino acids (i.e., phenylalanine, lysine, methionine) show minimal change and thus are reflective of the base of the food web (McClelland and Montoya 2002, Chikaraishi et al. 2009, Ohkouchi et al. 2017).

Similar to the nitrogen stable isotope composition of amino acids as a proxy for nitrogen sources, carbon isotopic composition has emerged as a useful tool for assessing historic changes in phytoplankton (McMahon et al. 2015, Larson et al. 2013, Lorrain et al. 2019). However, cellular growth rates, phytoplankton community composition, the isotopic composition of carbon in CO_2, and CO_2 concentration all affect the $\delta^{13}C$ ($^{13}C/^{12}C$) values of phytoplankton in tandem (Lorrain et al. 2019, Montoya 2007, Burkhardt et al. 1999). The relative effects of these factors remain difficult to discern from carbon isotope data alone. Nonetheless, carbon stable isotope data is highly correlated with copepod biomass in the northeast Pacific and thus can be a useful combined index of ocean productivity (Espinasse et al. 2020). While both source amino acid

92 $\delta^{15}N$ and bulk $\delta^{13}C$ values can be influenced by a number of biogeochemical and physiological
93 processes (Figure 1), they are useful indicators of nitrogen utilization (source amino acid $\delta^{15}N$)
94 and phytoplankton dynamics (bulk $\delta^{13}C$), despite the difficulty in identifying specific
95 mechanisms of fractionation.
96 Here we use source amino acid $\delta^{15}N$ and bulk $\delta^{13}C$ values of consumer bone collagen as
97 indicators of change in food web-assimilated nitrogen (nitrogen utilization and isotopic
98 composition at the base of the food web) and food web-assimilated production (phytoplankton
99 composition, [CO_2], cellular growth, and physiology). These definitions assume major changes
100 in nitrogen utilization and phytoplankton dynamics are recorded in the stable isotope
101 composition of nitrogen and carbon in phytoplankton (McMahon et al. 2019, Sherwood et. al.
102 2011, de la Vega 2020, Ohkouchi et al. 2017), scaled to the spatial and temporal resource use of
103 consumers, and conserved with minimal trophic fractionation (Chikaraishi et al. 2009). Bulk
104 $\delta^{13}C$ and $\delta^{15}N$ values of source amino acids such as phenylalanine ($\delta^{15}N_{Phe}$) from long-lived,
105 generalist consumers provide ecosystem-level information of carbon and nitrogen dynamics that
106 are integrated over space, time, and multiple energy pathways in the food web (McCann et al.
107 2005; Rooney et al. 2006, de la Vega et al. 2020). As a result, these data sources are more
108 relevant to questions of food web responses to large-scale environmental forcing than discrete
109 measurements of inorganic nutrients or phytoplankton. Ultimately these data can be used to
110 understand how ecosystems have responded to environmental variability in the past and glean
111 insights into food web responses to oceanic conditions in the future.
112 Harbor seals (*Phoca vitulina*) are a particularly well-suited predator to understand food
113 web shifts through time because of their primarily piscivorous diet, generalist foraging strategies,
114 high site fidelity, and frequent occurrence in museum specimen collections. Adult harbor seals
115 typically forage 5 - 10 km from haul out sites and at depths < 200 m (Lowry et al. 2001) and are
116 opportunistic feeders (Lance et al. 2012). Therefore, the nitrogen and carbon stable isotope
117 composition of harbor seals offer a robust representation of the isotopic composition of carbon
118 and nitrogen assimilated into coastal food webs. Harbor seal specific trophic enrichment factors
119 for nitrogen have been quantified in controlled feeding studies, confirming minimal trophic
120 enrichment for phenylalanine between seals and their prey (Germain et al. 2014).
121 Environmentally induced shifts in foraging patterns, specifically nearshore verse offshore
122 feeding, has the potential to affect the carbon isotope composition in harbor seal tissues (Figure

1). We assume these behavioral effects are minimal on annual time scales compared to changes in the carbon and nitrogen isotope composition at the base of the food web given their restricted foraging ranges.

We aim to identify how archived $\delta^{15}N_{Phe}$ and bulk $\delta^{13}C$ values vary regionally across the northeast Pacific on ecologically relevant scales (integrated annually and regionally) and through time using museum harbor seal specimens from 1928-2014 (Figure 2). Additionally, we characterize abiotic factors that influence harbor seal $\delta^{15}N_{Phe}$ and bulk $\delta^{13}C$ values to identify ocean conditions important for food web assimilation of nitrogen and carbon. The effect of regional ocean condition on the stable isotope signature of source amino acids limits the application of short-term datasets for productivity studies, as short-term environmental perturbations are difficult to decouple from longer term trends such as climate regimes (Vokhshoori and McCarthy 2014). We therefore identify long-term environmental drivers that are important for interpreting reconstructed isotope data.

Materials and Methods

Sample Collection and Analysis

Harbor seal bone samples were obtained from specimens curated at the Burke Museum (University of Washington), the Slater Museum (University of Puget Sound), the Museum of the North (University of Alaska Fairbanks), the Royal British Columbia Museum, the Smithsonian Institute, and the National Marine Mammal Laboratory (NOAA) (*SI2, Table S1*). Specimens were either treated by maceration in warm water or cleaned by beetles and soaked in a dilute ammonia solution then stored in acid free boxes. Adult specimens were sampled from three regions: eastern Bering Sea, the Gulf of Alaska, and Washington state, which also included 18 specimens from the southern British Columbia coast (Figure 2). We further stratified samples from the Gulf of Alaska into two subregions (northern and southeast) and Washington state into two subregions (coastal and Salish Sea) for a total of five subregions. Sampling prioritized long-term temporal coverage, specifically focusing on climate regimes shifts (i.e., PDO). Additionally, samples with sex and size metadata were prioritized, although it was not available for most specimens. Metadata was accessed through VertNet using catalogue numbers and institution codes (http://www.vertnet.org/index.html).

Bone samples were decalcified with the resulting collagen acid hydrolyzed, derivatized, and analyzed for compound-specific nitrogen stable isotope analysis (CSSIA) of 11 individual

amino acids, including one source amino acid, phenylalanine (phe). Of the 11 amino acids, phenylalanine was the only discernable source amino acid and phenylalanine is the only amino acid data are reported in this manuscript (*Appendix S1*). CSSIA samples were analyzed by GC-C-irMS at the University of Washington Facility for Compound-Specific Stable Isotope Analysis of Environmental Samples using a Thermo Scientific Trace GC + GC IsoLink coupled to a Delta V irMS following the procedures developed by Chikaraishi et al. (2007) and protocols by Rachel Jeffrey's lab at University of Liverpool UK (full analytical details are provided in *Appendix 1*). Individual collagen samples were analyzed in triplicate along with a mixed amino acid standard of known isotopic composition (Sigma-Aldrich Co.) (mean precision of analytical standard for phenylalanine = 0.3‰). Internal and external standards were used and data processing included a drift correction. A total of 215 specimens were sampled from the time period of 1928-2014 for CSSIA, making this the largest CSSIA dataset of a mammal to date. Decalcified collagen of 190 specimens was analyzed for bulk $^{13}C/^{12}C$ and bulk $^{15}N/^{14}N$ at the University of Washington's IsoLab using a Costech ElementalAnalyzer, ConFlo III, MAT253 for continuous flow-based measurements. $^{15}N/^{14}N$ and $^{13}C/^{12}C$ are reported in standard delta notation:

$$1.\ \delta^{15}\mathrm{N}\ (\text{‰ vs. air}) = \left(\frac{(^{15}\mathrm{N}/^{14}\mathrm{N})_{\mathrm{Sample}}}{(^{15}\mathrm{N}/^{14}\mathrm{N})_{\mathrm{Air}}} - 1\right) * 1000$$

$$2.\ \delta^{13}\mathrm{C}\ (\text{‰ vs. VPBD}) = \left(\frac{(^{13}\mathrm{C}/^{12}\mathrm{C})_{\mathrm{Sample}}}{(^{13}\mathrm{C}/^{12}\mathrm{C})_{\mathrm{VPBD}}} - 1\right) * 1000$$

Internal laboratory standards (Bristol Bay salmon and glutamic acid) were interspersed with samples for a two-point calibration and blank correction (mean standard precision 0.09‰ for $\delta^{15}N$ and 0.04‰ for $\delta^{13}C$). A linear drift correction was also applied using IsoDat software. The collagen C:N ratio was used to verify the integrity of collagen for stable isotope analysis following specimen treatment and storage (van Klinken 1999).

The isotopic composition of marine dissolved organic carbon has been steadily depleted in ^{13}C over the past 100 years due to increases in anthropogenic CO_2 in the atmosphere (referred to as the Oceanic Seuss Effect) (Quay et al. 1992). $\delta^{13}C$ data were therefore corrected for the Seuss Effect using the following equation (Misarti et al. 2009):

$$3.\ \text{Suess Effect Correction Factor} = \mathrm{d} * \mathrm{e}^{\,0.027\,*\,(\mathrm{t}\,-\,1850)}$$

Where *d* is the maximum annual rate of $\delta^{13}C$ decrease specific to the North Pacific (-0.014 derived from Quay et al. 1992) *t* is the year represented by the year of specimen collection with a

one-year lag. The Seuss effect varies regionally (Tagliabue and Bopp 2008) and we applied a northeast Pacific parameterization (Misarti et al. 2009).

Standard linear models were used to identify whether size (standard length, cm), sex, and subregion of the harbor seals sampled were related to isotopic composition and to test whether these parameters needed to be standardized in environmental models. $\delta^{15}N_{Phe}$ and $\delta^{13}C$ values were modelled independently as univariate continuous response variables using the following equation:

$$4.\ y_i \sim N(\alpha + \boldsymbol{\beta}\mathbf{X}_i,\ \sigma_y^2)$$

where y is the mean triplicate value for each individual i for either $\delta^{15}N_{Phe}$ or $\delta^{13}C$ values. $\boldsymbol{X}$ represents the matrix of predictors (sex, length, subregion), α is a scalar and $\boldsymbol{\beta}$ is a vector of coefficients for the predictors. Length (n = 116) was modelled as a continuous variable and was natural log transformed; subregion and sex (n = 190) were modelled as factors. Individual models were used to test whether a predictor was significant as opposed to a multivariate framework because, 1) sample sizes for $\delta^{15}N_{Phe}$ (n = 215) and $\delta^{13}C$ (n = 190) data varied, and 2) predictor metadata was incomplete for specimens. A pairwise t-test using the Bonferroni correction and non-pooled standard deviation was also used to compare differences in mean isotope signature between subregions and sex (Figure 3, *Tables S3 & S4*).

To understand the extent of coupling between indices of food web assimilated production and nitrogen resources, a linear model representing the basin wide relationship was fit to $\delta^{13}C$ and $\delta^{15}N_{Phe}$ values as continuous variables assuming normal errors. To understand spatial variation in this relationship, a hierarchical model was fit to the same dataset with varying slope and varying intercept based on subregion as a random effect. This model took the following form:

$$5.\ y_i \sim N(\boldsymbol{\alpha}_{j[i]} + \boldsymbol{\beta}_{j[i]}\mathbf{x}_i,\ \sigma_y^2)$$

Where y represents $\delta^{13}C$ values as a continuous variable and x represents $\delta^{15}N_{Phe}$ values as a continuous variable and j represents the group level predictor, subregion. $\boldsymbol{\alpha}$ and $\boldsymbol{\beta}$ are each vectors of coefficients that vary by subregion.

Quantifying effects of ocean condition on food web isotope indices

Linear models were used to identify environmental drivers of $\delta^{13}C$ and $\delta^{15}N_{Phe}$ values using a suite of environmental indices as covariates. A total of 42 environmental time series were compiled as potential predictor variables (*Table S1*) based on previous evidence for food web

214 importance in the northeast Pacific (sensu, Stachura et al. 2014, Di Lorenzo et al. 2008). Each
215 environmental time series was standardized around a mean of 0 and standard deviation of 1 and
216 discharge data was also natural log transformed. We divided these environmental covariates *a*
217 *priori* into four main mechanistic properties based on the expected effect on nutrient assimilation
218 into the food web: climate regime, freshwater discharge, circulation (wind and upwelling), and
219 sea surface temperature (Figure 1). Given the three regions in our analysis, each of these
220 hypotheses were also divided according to our regional geographic breaks (eastern Bering Sea,
221 Gulf of Alaska, and Washington). To reduce collinearity between environmental time series and
222 reduce the total number of candidate models, a subset of 7 environmental times series were
223 selected for each region based on the temporal overlap with stable isotope data. Each subset
224 contained at least one time series for each of the four mechanistic properties and all possible
225 combinations of predictors were tested (*Table S2*). While reduction of the number of times series
226 provides analytical benefits, it comes at the cost of potentially conservative estimates of which
227 covariates are important, meaning important components of ocean condition to the food webs
228 may be missed.
229 $\delta^{15}N_{Phe}$ and $\delta^{13}C$ values were independently considered as response variables to evaluate
230 relationships between predictors (environmental indices and location) and stable isotope data
231 using equation 4 where $\boldsymbol{X}$ is a matrix of predictors using the 7 standardized environmental time
232 series (continuous) and subregion (factor) as covariates. We treated carbon and nitrogen isotopes
233 as response variables separately in linear models, rather than in a combined multivariate model
234 due to differences in sample size and differences in the strength of correlation between for
235 $\delta^{15}N_{Phe}$ and $\delta^{13}C$ values for each subregion. Time series data prior to 1950 and after 2014 was
236 excluded from this analysis as data for some covariates did not extend beyond 1950. Candidate
237 models (n = 53) were compared using Akaike Information Criteria with a small sample size
238 correction (AIC_c, Akaike 1973) and included all combinations of the environmental indices. In
239 addition, a subregion factor was included with two levels for Washington (Salish Sea and coastal
240 Washington) and the Gulf of Alaska (southcentral and southeast) and a null model (intercept
241 only) was also tested. Tissue turnover time of bone collagen has not been measured in mammals
242 of this size to our knowledge but is approximately 173 days for birds (Hobson and Clark 1992).
243 Thus, a lag of one year was applied to the stable isotope datasets to account for the timing of
244 tissue turnover in bone collagen (additional lags were also considered, see *Appendix S2*). For

each model with relatively high support ($\Delta AIC_c < 2$) the AIC_c weight and the coefficient for each covariate is reported (Figure 3). To confirm collinearity was not problematic in the candidate models that included more than one environmental covariate, matrix scatterplots and variance inflation factors (vif) were used from the car package (Fox and Weisberg 2019) in R (R Development Core Team, 2020).

Gaussian Process Dynamic Factor Analysis (GPDFA)

To further understand how the environment, $\delta^{13}C$, and $\delta^{15}N_{Phe}$ values covary through time in the Northeast Pacific, we developed a novel extension of conventional Dynamic Factor Analysis (DFA). DFA is a dimension reduction technique that identifies common processes underlying a set of multivariate time series. This technique has been applied to multivariate time series problems in fisheries and ecology to identify patterns of oceanographic variability that drive Pacific salmon stocks (Stachura et al. 2014, Jorgenson et al. 2016, Ohlberger et al. 2016).

DFA models identify common trends across multiple time series ("latent trends") and estimates the importance of that trend for each individual time series as a coefficient ("factor loading"). The two equations describing DFA take on the following form:

6. $\mathbf{y}_t = \mathbf{Z}\mathbf{x}_t + \mathbf{v}_t$, where $\mathbf{v}_t \sim \text{MVN}(0, \mathbf{R})$

7. $\mathbf{x}_t = \mathbf{x}_{t-1} + \mathbf{w}_t$, where $\mathbf{w}_t \sim \text{MVN}(0, \mathbf{I})$

The observed data $\mathbf{y}_t$ are modeled as combinations of latent trends $\mathbf{x}_t$ at time *t* (the dimensions of $\mathbf{x}_t$ matching the number of trends which are also referred to as states) and factor loadings ($\mathbf{Z}$) (a coefficient for each time series for each trend) at time *t,* which are modeled as a random walk (Zuur et al. 2003). In addition there is an optional random observation error ($\mathbf{v}_t$) and process error ($\mathbf{w}_t$) which are multivariate normal

Our extension of DFA adopts an alternative model of the latent trends, modeling them with Gaussian Processes rather than random walks (*Appendix 3*). With conventional DFA using an autoregressive model, long gaps in time series data result in large, overestimations of the variance of the latent trends. Gaussian Processes model time series as a multivariate normal distribution, with estimated mean vector $\boldsymbol{u}$ and covariance matrix $\boldsymbol{\Sigma}$ (Munch et al. 2018). To constrain the number of estimated parameters, elements of $\boldsymbol{\Sigma}$ were modeled with a Gaussian or squared covariance exponential function such that $\Sigma_{i,j} = \sigma^2 \exp\left(-(t_i - t_j)^2/\theta\right)$. In this parameterization, σ^2 controls the variability of the stochastic process, θ controls the rate of decay

in correlation between time steps, and t_i and t_j are the time variables (e.g. years) for locations *i* and *j*.

We considered models with 1- 4 underlying trends. Each trend was modelled separately (different means) but models with multiple trends to have a shared covariance matrix amongst trends. The GPDFA approach was applied to time series from each region and the best model was selected using leave-one-out cross-validation (LOOIC) from the loo package in R (Vehtari et al. 2017). The choice of knots affects the degree of smoothness, with more knots creating more smooth functions. We tested several different numbers of knots and found results to be qualitatively similar. Similar to the previous analysis, time series data prior to 1948 for Washington state and prior to 1940 and after 2008 for the Gulf of Alaska was excluded from this analysis. We fit GPDFA to data from each region including all of the initial 42 identified environmental time series for that region (*Table S1*), $\delta^{15}N_{Phe}$ and $\delta^{13}C$ values, with location as a factor. We implemented GPDFA using the Stan language (Stan Development Team 2019, Carpenter et al. 2017), and R (R Core Development Team 2019, version 3.6.2) via R package rstan (Stan Development Team 2019, version 2.21.2). Code to implement GPDFA is available here: https://github.com/mfeddern/CSIA-AA/blob/master/SourceData/Src/Analysis/gpdfa.stan

Results

$\delta^{15}N_{Phe}$ and bulk $\delta^{13}C$ values did not vary by sex ($p > 0.05$, Figure 3) or size for the individuals sampled ($p > 0$ .05; *Figure S2*). Spatial variation in harbor seal $\delta^{15}N_{Phe}$ and $\delta^{13}C$ values were observed on subregional scales. $\delta^{15}N_{Phe}$ values were similar for harbor seals in the northern Gulf of Alaska (11.9 ± 2.9, mean ± 1SD), southeast Gulf of Alaska (10.8 ± 1.7), and coastal Washington (11.3 ± 1.9). The eastern Bering Sea had significantly higher $\delta^{15}N_{Phe}$ values compared to other subregions (15.2 ± 1.8) followed by the Salish Sea (12.2 ± 2.3) which had similar $\delta^{15}N_{Phe}$ values compared to the northern Gulf of Alaska (Figure 3, *Table S3*). $\delta^{13}C$ values varied by subregion ($p < 0.05$) with the exception of the Gulf of Alaska, where the northern (-14.6 ± 0.9) and southeast (-14.4 ± 1.1) subregions were not significantly different, and the eastern Bering Sea (-13.4 ± 0.9) and coastal Washington (-13.6 ± 0.9) were not significantly different (Figure 3, *Table S4*). The variation between subregions appeared to follow a latitudinal gradient, where harbor seal mean $\delta^{13}C$ values were most enriched in ^{13}C in the Salish Sea (-12.2 ± 1.5), became more depleted from coastal Washington and into the Gulf of Alaska (Table 1).

The relationship between harbor seal $\delta^{15}N_{Phe}$ and $\delta^{13}C$ values also varied on subregional scales. There was positive linear association between harbor seal $\delta^{15}N_{Phe}$ and $\delta^{13}C$ values in the combined northeast Pacific basin and Bering Sea model with a slope of 0.12 (Figure 4A). For the hierarchical subregion model, the eastern Bering Sea and coastal Washington demonstrated similar relationship, with slopes of 0.08 (95% CI [0.05, 0.11]) and 0.07 (95% CI [0.05, 0.09]) respectively. Similarly, harbor seals in both Gulf of Alaska subregions demonstrated comparable coupling of $\delta^{15}N_{Phe}$ and $\delta^{13}C$, with slopes of 0.13 (95% CI [0.11, 0.14]) for the northern subregion and 0.12 (95% CI [0.10, 0.14]) for the southeastern subregion. Salish Sea harbor seals had a distinct relationship between $\delta^{13}C$ and $\delta^{15}N_{Phe}$ values relative to other subregions with a slope of only 0.02 that was not significantly different from 0 (95% CI [0.0, 0.04]) (Figure 4B).

For both $\delta^{15}N_{Phe}$ and $\delta^{13}C$ values there was substantial support for models including environmental indices rather than null or subregion only models. The relationship between environmental indices and harbor seal $\delta^{13}C$ and $\delta^{15}N_{Phe}$ values in the northeast Pacific varied on regional scales. For Washington, the best model to predict harbor seal $\delta^{15}N_{Phe}$ values included Columbia River discharge in high flow months, summer upwelling, and subregion. There was substantial model uncertainty for $\delta^{15}N_{Phe}$ values in the Washington region, however 90% of model weight supported the inclusion of Columbia River discharge (Figure 5A). The model for harbor seal $\delta^{13}C$ values with the most support indicated a positive association between PDO, spring upwelling, and freshwater discharge in the Washington region (Figure 5B). In the Gulf of Alaska, the summer upwelling model had the most support as a predictor of harbor seal $\delta^{15}N_{Phe}$ values with some model support for inclusion of the NPGO (North Pacific Gyre Oscillation), although the coefficients for this covariate did not differ substantially from 0 (Figure 5C). The best model for harbor seal $\delta^{13}C$ values for the Gulf of Alaska included subregion, PDO (Pacific Decadal Oscillation), and NPGO (Figure 5D). In contrast to Washington, the Gulf of Alaska models supported a negative association between $\delta^{13}C$ values and PDO. The null model for $\delta^{15}N_{Phe}$ values in the eastern Bering Sea had the most support (Figure 5E). Lack of model support for environmental covariates in the eastern Bering Sea may have been a result of the small sample size in the region. Cross-shelf wind was included as a predictor in the best model (Figure 5F) for $\delta^{13}C$ values in the eastern Bering Sea and was supported by 76% of the model weight.

PDO and Kuskokwim river discharge during high flow months were found to be highly collinear (VIF > 10) and PDO was omitted from the candidate model set for the eastern Bering

Sea analysis. All other models containing multiple environmental predictors with relative support had variance inflation factors of less than 2 indicating only moderate collinearity across covariates. Model residuals for the best models did not show trends through time (*Figure S7*). This indicates that there were no trends associated with other potential ecosystem changes, such as harbor seal foraging strategy for example, after accounting for ocean condition. Model results did not change when using $\delta^{13}C$ data that were not corrected for the regional Seuss Effect.

The GPDFA analysis showed temporal synchronies and shared trends across environmental conditions and stable isotope values in the northeast Pacific. In the Gulf of Alaska, the data supported three latent trends (Figure 6). Both $\delta^{15}N_{Phe}$ and $\delta^{13}C$ values had the highest loadings for trend 1, which showed an increase starting in 1965 until 1980 followed by the trend oscillating at approximately 25% above the long-term average. The harbor seal $\delta^{15}N_{Phe}$ values for the southeast subregion, harbor seal $\delta^{13}C$ values, and spring upwelling had negative loadings on trend 1; loadings of $\delta^{15}N_{Phe}$ values were generally weaker relative to loadings of $\delta^{13}C$ values. For the other two trends (2-3), loadings were clustered by environmental driver category. Latent trend 2 oscillated around the long-term average and was uninformative. Trend 3 was below average starting in 1985 with strong loadings for climate time series, spring and summer upwelling, and discharge in high flow months (Figure 6). Annual discharge, autumn upwelling, Oceanic Niño Index and Northern Oscillation Index did not demonstrate strong loadings for any trend. In Washington, there was support for two latent trends. Latent trend 1 shows a rapid increase in the 1940's to 25% above the long-term mean then a gradual decline until 1986 to approximately 40% below the long-term mean, with values below the mean starting in 1977 (Figure 7). Trend loadings for harbor seal $\delta^{15}N_{Phe}$ and $\delta^{13}C$ values were stronger for coastal seals and trend 1 had stronger loadings for freshwater discharge than trend 2. Trend 2 had strong loadings for $\delta^{15}N_{Phe}$ and $\delta^{13}C$ values for both Salish Sea and coastal Washington harbor seals. Trend 2 oscillated above and below the long-term mean and had large loadings for sea surface temperature, summer upwelling, Fraser River discharge and climate indices (Figure 7).

Discussion

We analyzed bone collagen $\delta^{15}N_{Phe}$ and bulk $\delta^{13}C$ values from harbor seal museum specimens collected between 1928 and 2014 as indices of change in food web assimilated nitrogen and carbon. Based on previous research (i.e., Graham et al. 2010, Sherwood et al. 2014, de la Vega et al. 2019, Lorrain et al. 2019, de la Vega et al. 2020), we interpret $\delta^{15}N_{Phe}$ and bulk

$\delta^{13}C$ values as primarily representing nitrogen and carbon resource utilization, and growth and community composition of primary producers at the base of the food web. Our data show the relationship between indices of primary production and nitrogen resources assimilated into food webs varies regionally across the northeast Pacific. By pairing these data with environmental time series data, we provide new insights into large scale environmental forcing that impacts the base of the food web and is transferred to higher trophic levels. Specifically, oceanic conditions associated with climate regimes and upwelling explain significant temporal variation in $\delta^{15}N_{Phe}$ and bulk $\delta^{13}C$ values of coastal predators in northeast Pacific (Figure 5; *Figure S7*). This analysis demonstrates $\delta^{15}N_{Phe}$ and bulk $\delta^{13}C$ values are useful indicators of resources assimilated by coastal food webs.

Spatial variation in stable isotope indices

The geographically widespread association between harbor seal $\delta^{15}N_{Phe}$ and $\delta^{13}C$ values indicates food web assimilated primary production is coupled with nitrogen resources in most regions of the northeast Pacific, with the Salish Sea as a notable exception (Figure 4). Short-term studies in coastal Washington showed phytoplankton respond considerably to nitrogen inputs and are frequently nitrogen limited (Dortch and Postel 1989, Kudela and Peterson 2009). Similarly, short term studies of the inner Gulf of Alaska shelf demonstrated primary production is generally nitrogen limited, and size, growth rates, and community composition are all tightly coupled with nutrient availability (Strom et al 2006). A significant relationship between bulk $\delta^{15}N$ and $\delta^{13}C$ values was also observed in the tissues of some gorgonian corals over the same time period in coastal Gulf of Alaska (Williams et al. 2007). Given the evidence of nitrogen limitations and its relationship with phytoplankton growth and community composition in these coastal environments, the association between $\delta^{15}N_{Phe}$ and $\delta^{13}C$ values could be the result of nitrogen limiting growth at the base of the food web. Alternatively, the $\delta^{15}N_{Phe}$ and $\delta^{13}C$ coupling could be driven by covariance with an untested environmental variable that impacts most of the northeast Pacific but not the Salish Sea.

The coastal Washington and the Salish Sea food webs assimilate different nitrogen and carbon sources (Figure 5A & B). Salish Sea harbor seals have higher $\delta^{15}N_{Phe}$ and $\delta^{13}C$ values compared to individuals on the outer coast, which is likely due to significant contributions of intertidal producers and the legacy of anthropogenic N in the Salish Sea food web. Intertidal macrophytes (seagrass and algae) have similar $\delta^{13}C$ values (~ -10‰) compared to harbor seals in

398 the Salish Sea, while other potential sources are much lower (i.e., marine derived sources ~ -
399 20‰, terrestrial derived sources ~ -30‰) (Conway-Cranos et al. 2015, Howe and Simenstad
400 2015). Incorporation of intertidal producers into the Salish Sea food web explains the difference
401 in carbon stable isotope signatures between Salish Sea and coastal Washington harbor seals
402 (~1.4‰, Figure 5A). However, it does not explain the higher $\delta^{15}N_{Phe}$ values (Figure 5B, Table 1).
403 Surface nitrate was observed to be 8‰ – 12‰ off the coast of Washington in spring 1993 (Wu et
404 al. 1997) which was exceeded by harbor seals in both coastal Washington and the Salish Sea
405 (Table 1). It is likely anthropogenically derived nitrogen sources contribute to the higher
406 observed $\delta^{15}N_{Phe}$ values both directly and indirectly, particularly in the Salish Sea where harbor
407 seal $\delta^{15}N_{Phe}$ values were up to 2.4‰ higher than coastal Washington seals. Wastewater treatment
408 facilities and agriculture runoff contribute substantial amounts (~32%) of nitrogen in the Salish
409 Sea (Mohamedali et al. 2011) and are enriched in ^{15}N. In recent decades, Salish Sea waters have
410 also been characterized by low dissolved oxygen and hypoxic events (PSEMP 2019) from
411 human derived nitrogen loading. Anoxic conditions are conducive to denitrification, another
412 potential indirect source of ^{15}N from human activities in the region.
413 *Ocean condition and stable isotope indices*
414 Washington state food webs exhibit environmentally induced changes in assimilated
415 primary production and nitrogen sources. The isotope-ocean condition relationship in the region
416 can be explained by introduction of terrestrial derived nutrients and climatically induced changes
417 in phytoplankton community structure observed in previous studies (Du et al. 2015, Du and
418 Peterson 2014, Kudela et al. 2008). For example, the PDO has been associated with
419 phytoplankton community shifts between dinoflagellates and diatoms in the northern California
420 Current (Du et al. 2015). Similarly, the phytoplankton community composition is distinct in the
421 early (spring) upwelling season compared to the late (summer) upwelling season (Du and
422 Peterson 2014). This could explain the inversely related associations between $\delta^{13}C$ values and
423 summer and spring upwelling (Figure 5B). Shifts in phytoplankton community structure are
424 therefore a mechanism to explain the relationship between harbor seal $\delta^{13}C$ values and ocean
425 condition. In addition, freshwater discharge explains 16% of variation observed in both $\delta^{15}N_{Phe}$
426 and $\delta^{13}C$ values in Washington. The Columbia River Plume introduces terrestrial derived
427 nutrients, including nitrogen, and has been associated with increased primary production and fish
428 production (Kudela et al. 2008, Ware and Thomson 2005). The covariation between $\delta^{15}N_{Phe}$,

429 $\delta^{13}C$, and discharge indicates isotopically distinct nitrogen resources introduced by freshwater
430 discharge alters primary production which is then assimilated into the Washington food web, and
431 ultimately harbor seals.
432 In the eastern Bering Sea, our results suggest ice-born algae and ^{15}N enriched nitrogen
433 from the inner shelf are important for supporting the coastal food web. Recent evidence supports
434 that consumer $\delta^{15}N_{Phe}$ values reflect nitrate $\delta^{15}N$ values in the arctic (de la Vega et al. 2020).
435 However, our $\delta^{15}N_{Phe}$ values from harbor seals of the eastern Bering Sea were high relative to
436 previous studies of summer nitrate (5 to 9‰, Lehmann et al. 2005) and plankton nitrogen isotope
437 signatures (6-12‰, Smith et a. 2002) from the outer and mid Bering Sea shelf. Morales et al.
438 (2014) subsequently found the stable isotope composition of nitrogen in diatoms ranged from 5-
439 21‰ in late winter and early spring. These values also increased in association to sea ice with a
440 positive shoreward gradient (Morales et al. 2014). The range of sea-ice algae $\delta^{15}N$ values
441 observed by Morales et al. (2014) are consistent with our observed $\delta^{15}N_{Phe}$ values in harbors seals
442 (Table 1). Furthermore, the harbor seals in this study were located near the inner shelf in an area
443 that has been partially covered by sea ice from January to May during the past century (Stabeno
444 et al. 2007). Together this indicates ice algae as a significant contributor to the coastal food web.
445 The disconnect between the $\delta^{15}N$ values of offshore nitrate (Lehmann et al. 2005) and harbor
446 seals also highlights the problem in assuming spatially and temporally discrete nitrate or
447 phytoplankton measurements are representative of resources utilized by, and assimilated into,
448 coastal food webs. Consumer $\delta^{15}N_{Phe}$ measurements by their nature represent the N assimilated
449 into the food web and integrated over relatively long time scales, while discrete measurements of
450 nitrate may be spatially or temporally biased.
451 A short term (1998-2011) study of abiotic drivers in the Gulf of Alaska found
452 chlorophyll-a anomalies were positive when downwelling favorable winds were low and had a
453 negative relationship with sea level (Waite and Mueter 2013). Similarly, Espinasse et al. (2020)
454 found chlorophyll-a, SST, and sea level anomalies were the best predictors of carbon and
455 nitrogen isotope data for secondary consumers over the past two decades. Our results agree with
456 these studies as NPGO (an index of sea level) is negatively associated with both harbor seal
457 $\delta^{15}N_{Phe}$ (Figure 5C) and $\delta^{13}C$ values (Figure 5D) in the Gulf of Alaska. Similarly, summer
458 upwelling is positively associated with our $\delta^{15}N_{Phe}$ values (Figure 5C). Based on our results,
459 these environmentally induced changes represent long-term ecosystem dynamics that extend

beyond merely the base of the food web and ultimately impact resources assimilated by top predators. In addition, regional climate indices characterize nutrient and primary production assimilated annually into the food web better than sea surface temperature data alone. It is possible that other untested abiotic factors such as cross-shelf exchanges via eddy propagation or local wind stress (Waite and Mueter 2013) may be important to food web assimilated nitrogen and primary production in the Gulf of Alaska. Regardless, local variability in upwelling and basin scale indices of sea surface height and temperature (i.e., NPGO) ultimately determine resource assimilation in Gulf of Alaska food web in which harbor seals forage.

By comparing consumer stable isotope values against environmental covariates across multiple sub basins we show environmental forcing on coastal food webs is regionally distinct. For example, climate indices (i.e., PDO) in the Gulf of Alaska were inversely associated with food web-assimilated primary production (Figure 5D, Figure 6 Trend 1-2) and positively associated in Washington (Figure 5B, Figure 7 Trends 1-2). This agrees with previous studies where the Pacific Decadal Oscillation has been associated with alternating salmon production in the northeast Pacific (Mantua et al. 1997, Mantua and Hare 2002). In cool phase years (i.e., 1947-1977), Washington stocks experience above average production and Alaska stocks experience below average production. Our results show that $\delta^{13}C$ values for Washington and Gulf of Alaska also indicate alternating primary production between the two regions in association with PDO. Surprisingly, $\delta^{13}C$ values are higher in cool phase years for the Gulf of Alaska (Figure 5D) and lower in cool phase years for Washington (Figure 5B). This suggests there is lower phytoplankton growth in Washington and higher in Gulf of Alaska in cool phase years. This is contrary to results of previous studies, assuming 1) higher $\delta^{13}C$ values represent higher growth rates and 2) PDO is inhibiting growth at the base of the food web and indirectly constraining higher trophic levels such as salmon (Mantua et al. 1997, Mantua and Hare 2002). It is likely the relationship between PDO, salmon production, and $\delta^{13}C$ values of harbors seals is instead caused by phytoplankton community structure constraining higher trophic levels rather than growth.

Common temporal trends in harbor seal stable isotopes and ocean condition empirically derived from the GPDFA analysis (Figures 6 & 7) show changes in biogeochemical cycling and food web-assimilated production in recent decades that are associated with climatic variables. Since 1975, shared trends in environmental time series and stable isotope data in the Gulf of

Alaska are above average for temperature, discharge, and NPGO and below average for assimilated $\delta^{13}C$ values (as indicated by its negative loadings; Figure 6). Trends 2 and 3 in the Gulf of Alaska (Figure 6) show a distinct change in environmental indices starting in 1988. Loadings on these trends were higher for environmental indices than stable isotope data, suggesting a decoupling of environment-food web relationship in the region starting around 1988, which has also been observed between climate regimes and fish species (Litzow et al. 2020). This environmental-food web decoupling was not observed in Washington (Figure 7) in our study or others (Litzow 2020).

Using stable isotopes as food web indicators

Previous research has shown lower trophic levels are sensitive to environmental variation in bottom-up drivers of productivity (sensu, Ware and Thompson 2005, Frank et al. 2015, Jennings and Brander 2010), but few studies have demonstrated how the impact of these changes span entire food webs on long time scales. By applying CSSIA to museum specimens of a generalist predators, we provide a novel piece of the ecological puzzle not previously available. First, these data provide a measure of changing nitrogen resources and phytoplankton dynamics that are spatially and temporally integrated for food web resource assimilation, rather than measuring the availability of inorganic nutrients or lower trophic level biomass and assuming an associated food web response. Dominant species of marine zooplankton exhibit selective foraging, particularly when resources are highly available (Meunier et al. 2015, Bi and Sommer 2020, Jungbluth et al. 2017, Boersma et al. 2015) thus discrete measures of resources are not necessarily representative of what is utilized by the food web. Second, studies directly measuring primary production are often temporally limited to short time scales and recent decades. CSSIA of historic specimens allows for retrospective analyses that span long time scales (Mathews and Ferguson 2014, McMahon et al. 2015, McMahon et al. 2019, Sherwood et al. 2011) and thus identify long-term environmental forcing on food webs.

Despite these benefits, CSSIA (and stable isotope analysis data more generally) is limited in its ability to discern different mechanistic processes for isotopic enrichment in observational studies. Multiple mechanisms of fractionation often operate in tandem (Figure 1) and can be both additive and subtractive. For example, both the isotopic composition of dissolved inorganic nitrogen sources (primarily NO_3^-, but also urea and NH_4^+) and the relative uptake of these sources impact the isotopic composition of nitrogen in primary producers (Graham et al. 2010,

Ohkouchi et al. 2017). As a result, these data on their own are limited in their ability to track exact mechanisms of fractionation and specific biogeochemical changes through time or space. Regardless, stable isotope signatures of nitrogen from source amino acids and bulk carbon can be used to trace variations in nitrogen sources at the base of the food web (i.e., Sherwood et al. 2014, de la Vega et al. 2020) and changes in phytoplankton dynamics (i.e., production; de la Vega et al. 2019, Lorrain et al. 2019) broadly. In addition, CSSIA of carbon is also emerging as reliable proxy for phytoplankton community composition (McMahon et al. 2015, Larsen et al. 2013). We also assume a constant and small trophic enrichment factor for both bulk $\delta^{13}C$ and $\delta^{15}N_{Phe}$ values. While trophic enrichment in $\delta^{13}C$ and $\delta^{15}N_{Phe}$ values is minimal (Hobson et al. 1996, Bocherens and Drucker 2003, Germain et al. 2013, Ohkouchi et al. 2017), and thus unlikely to impact overall correlations between datasets, it can produce enriched absolute isotope values and increased variation between observations (Nielsen et al. 2015), which was not accounted for in this study. Nonetheless, ours is among a number of supporting studies that show food webs are impacted by changing environmental conditions in the northeast Pacific (Cunningham et al. 2018, Puerta et al. 2019, Stachura et al. 2014).

Climate change will alter nutrient distributions and primary production throughout the worlds' oceans (Marinov et al. 2010, Kwiatkowski et al. 2017). Based on analysis of historical patterns of consumer isotopic variation with environmental forcing, we anticipate there will be region-specific spatial variability in how primary production and its dependent food webs respond to environmental change throughout the northeast Pacific over the next century. As environmental conditions (i.e., sea surface temperature, discharge, anthropogenic nitrogen) continue to change, so will resources available to and assimilated by food webs. Given both resource availability and community composition of resources impact the function and stability of food webs (Narwani and Mazumder 2012) it is likely that ecosystem interactions will change in response to environmentally induced shifts in resources. Understanding dynamics influencing food web responses to their environment is important, as it provides information useful for predicting climate change impacts to aquatic resources and the communities and economies that depend on them.

Acknowledgements

We would like to extend our deepest gratitude to our museum collaborators for permitting sampling and coordinating logistics. Specifically, we thank Jeff Bradley and Sharlene Santana of

the UW Burke Museum, Peter Wimberger and Gary Shugart of the Slater Museum, Link Olson and Aren Gunderson of the Museum of the North, Robert Delong of the National Marine Mammal Laboratory, Lesley Kennes and Gavin Hanke of the Royal BC Museum, and Darrin Lunde and John Ososky of the Smithsonian Institute. We thank Megan Stachura and Tom Royer for assistance with environmental datasets, and Chris Harvey and Jens Nielsen for helpful discussions and support. Hyejoo Ro and Karrin Leazer assisted in lab work. Mark Haught and Terry Rolfe assisted with GC/C/IRMS methods development, maintenance, and troubleshooting. This publication was funded in part by grants from Washington Sea Grant, University of Washington, pursuant to National Oceanic and Atmospheric Administration Award No. NA18OAR4170095 and NA19OAR4170360. This publication is partially funded by the Joint Institute for the Study of the Atmosphere and Ocean (JISAO) under NOAA Cooperative Agreement NA15OAR4320063, Contribution No. 2020-1116. Additional funding was provided by an internal grant from the Northwest Fisheries Science Center. The views expressed herein are those of the authors and do not necessarily reflect the views of NOAA or any of its sub-agencies.

568 **Tables**

569 **Table 1:** Range of $\delta^{15}N_{Phe}$ and $\delta^{13}C$ values observed in harbor seals for each of the five northeast
570 Pacific subregions.

	$\delta^{15}N_{Phe}$ (‰)	$\delta^{13}C$ (‰)
Coastal WA	6.0 – 15.8	-15.6 – -11.8
Salish Sea	5.9 – 18.2	-16.6 – -6.8
Northern Gulf of Alaska	6.2 – 21.5	-16.7 – -12.5
Southeast Gulf of Alaska	8.0 – 15.2	-17.3 – -12.1
Eastern Bering Sea	12.4 – 18.9	-15.0 – -12.1

571

572

573 **Figures**

574 **Figure 1:** Mechanisms of environmentally induced changes in resources (A-D) assimilated into
575 stable isotope ratios of primary producers (1-2), which are conserved when assimilated into
576 higher trophic levels in the food web (3).

577

578 **Figure 2:** Spatial and temporal distributions of northeast Pacific harbor seal specimens by
579 subregion analyzed for $\delta^{15}N_{Phe}$ and bulk $\delta^{13}C$ values. Subplot colors correspond to map locations
580 and x-axis (years) is the same for each subplot.

581

582 **Figure 3**: Variability in $\delta^{15}N_{Phe}$ and $\delta^{13}C$ values based on sub region and sex. * denotes a
583 significant difference in isotopic signature between males and females for that region (colors
584 correspond to Figure 2).

585

586 **Figure 4:** Relationship between nitrogen sources ($\delta^{15}N_{Phe}$) and primary production ($\delta^{13}C$)
587 assimilated into the food web for **A.** a single linear model for the combined data across the
588 northeast Pacific and eastern Bering Sea and **B.** a mixed effects model with random slope and
589 intercept by sub region (colors correspond to Figure 2).

590

591 **Figure 5:** Coefficients of environmental covariates for models with relative support ($\Delta AIC_c < 2$)
592 for harbor seal $\delta^{15}N_{Phe}$ and $\delta^{13}C$ values in three regions of the northeast Pacific: Washington,

593 Gulf of Alaska, and the eastern Bering Sea. Color indicates model support based on AIC_c weight,
594 points are the coefficient estimates for each environmental covariate included in an individual
595 model, and bars show two standard deviations from the coefficient estimate.
596
597 **Figure 6:** Common trends in environmental condition and food web assimilated stable isotope
598 values for the regional Gulf of Alaska gaussian-dynamic factor analysis model. The solid lines
599 represent the modelled trends, where 0 is the long-term average and 1 and -1 represent the
600 maximum and minimum possible values respectively; the dash line is the 90% credible interval.
601 Factor loadings can be interpreted as coefficients, representing the strength of association
602 between the modelled trend and each observed environmental time series (colors represent *a*
603 *priori* driver category). Values close to 0 mean the observed time series did not correlate to the
604 corresponding trend, while values close to 1 show the observed time series closely matched the
605 modelled trend. Negative loadings indicate an inverse relationship between the observed time
606 series and modelled trend. Stable isotope times series are modelled separately for the northern
607 (N. $\delta^{15}N_{Phe}$; N. $\delta^{13}C$) and southeast (S. $\delta^{15}N_{Phe}$; S. $\delta^{13}C$) subregions.
608
609 **Figure 7:** Common trends in environmental condition and food web assimilated stable isotope
610 values for the regional Washington gaussian-dynamic factor analysis model. Stable isotope times
611 series are modelled separately for the coastal (C. $\delta^{15}N_{Phe}$; C. $\delta^{13}C$) and Salish Sea (S.S. $\delta^{15}N_{Phe}$;
612 S.S. $\delta^{13}C$) subregions. See Figure 6 caption for further interpretation.
613 **References**
614 Akaike H. (1973). Information theory and the maximum likelihood principle. In: B.N. Petrov and
615 F. Cs ä ki (Eds), 2nd International Symposium on Information Theory. Akademiai Ki à
616 do, Budapest.
617 Bi R., Sommer U. (2020). Food quantity and quality interactions at phytoplankton-zooplankton
618 interface: chemical and reproductive responses in a calanoid copepod. *Frontiers in*
619 *Marine Science* **7**, 274.
620 Bjorkland R.H., Pearson S.F., Jeffries S.J., Lance M.M., Acevedo-Gutiérrez A., Ward E.J.
621 (2015). Stable isotope mixing models elucidate sex and size effects on the diet of a
622 generalist marine predator. *Marine Ecology Progress Series* **526**, 213-225.

623 Bocherens H., Drucker D. (2003). Trophic level isotopic enrichment of carbon and nitrogen in
624 bone collagen: case studies from recent and ancient terrestrial ecosystems. *International*
625 *Journal of Osteoarchaeology* **13**, 46-53.
626 Boersma M., Mathew K.A., Niehoff B., Schoo K.L., Franco-Santos R.M., Meunier. (2015).
627 Temperature driven changes in the diet preference of omnivorous copepods: no more
628 meat when it's hot? *Ecology Letters* **19**, 45-53.
629 Bopp L., Resplandy L., Orr J.C., Doney S.C., Dunne J.P., Gehlen M., Halloran P., Heinze C.,
630 Ilyina T., Séférian R., Tjiputra J., Vichi M. (2013). Multiple stressors of ocean
631 ecosystems in the 21sst century: projections with CMIP5 models. *Biogeoscinces* **10**,
632 6225-6245.
633 Bonan G.B., Doney S.C. (2018). Climate, ecosystems, and planetary futures: The challenge to
634 predict life in Earth system models. *Science* **359**, eaam8328.
635 Brander K. (2010). Impacts of climate change on fisheries. *Journal of Marine System* **79**, 389-
636 402.
637 Brietburg D., Levin L.A., Oschlies A., Grégoire M., Chavez F.P., Conley D.J., Garçon V.,
638 Gilbert D., Gutiérrez D., Isensee K., Jacinto G.S., Limburg K.E., Montes I., Naqvi
639 S.W.A., Pitcher G.C., Rabalais N.N., Roman M.R., Rose K.A., Seibel B.A., Telszewski
640 M., Yasuhara M., Zhang J. (2018). Declining oxygen in the global ocean and coastal
641 waters. *Science* **359**, eaam7240.
642 Burkhardt S., Riebesell U., Zondervan I. 1999. Effects of growth rate, CO_2 concentration, and
643 cell size on the stable carbon isotope fractionation in marine phytoplankton. *Geochimica*
644 *et Cosmochimica Acta* **63**, 3729-3741.
645 Carpenter B., Gelman A., Hoffman M.D., Lee D., Goodrich B., Betancourt M., Brubaker M.A.,
646 Guo J., Li P., Riddell A., (2017). Stan: A probabilistic programming language. *Journal of*
647 *Statistical Software* **76**, 1-37.
648 Chikaraishi Y., Kashiyama, Ogawa N.O., Kitazato H., Ohkoushi N. (2007). Metabolic control of
649 nitrogen isotope composition of amino acids in macroalgae and gastropods: implications
650 for aquatic food web studies. *Marine Ecology Progress Series* **342**, 85-90.
651 Chikaraishi Y., Ogawa N.O., Kashiyama Y., Takano Y., Suga H., Tomitani A., Miyashita H.,
652 Kitazato H., Ohkouchi N. (2009). Determination of aquatic food-web structure based on

653 compound-specific nitrogen isotopic composition of amino acids. *Limnology and*
654 *Oceanography Methods* **7**, 740-750.
655 Conway-Cranos L., Kiffney P., Banas N., Plummer M., Naman S., MacCready P., Bucci J.,
656 Ruckelshaus M. (2015). Stable isotopes and oceanographic modeling reveal spatial and
657 trophic connectivity among terrestrial, estuarine, and marine environments. *Marine*
658 *Ecology Progress Series* **533**, 15-28.
659 Corwith H.L., Wheeler P.A. (2002). El Niño related variations in nutrient and chlorophyll
660 distributions off Oregon. *Progress in Oceanography* **54**, 361-380.
661 Cunningham C.J., Westley P.A.H., Adkinson M.D. (2018). Signals of large scale climate drivers,
662 hatchery enhancement, and marine factors in Yukon River Chinook salmon survival
663 revealed with a Bayesian life history model. *Global Change Biology* **24**, 4399-4416.
664 de la Vega C., Jeffreys R.M., Tuerena R., Ganeshram R., Mahaffey C. (2019). Temporal and
665 spatial trends in marine carbon isotopes in the Arctic Ocean and implications for food web
666 studies. *Global Change Biology* **25**, 4116-4130.
667 de la Vega C., Mahaffey C., Tuerena R.E., Yurkowski D.J., Yurkowski D.J., Ferguson S.H.,
668 Stenson G.B., Nordøy E.S., Haug T., Biuw M., Smout S., Hopkins J., Tagliabue A., Jeffreys
669 R.M. (2020). Arctic seals as tracers of environmental and ecological change. *Limnology and*
670 *Oceanography Letters*, doi: 10.1002/lol2.10176
671 Di Lorenzo E., Schneider N., Cobb K. M., Chhak, K, Franks P. J. S., Miller A. J., McWilliams J.
672 C., Bograd S. J., Arango H., Curchister E., Powell T. M. and P. Rivere. (2008). North
673 Pacific Gyre Oscillation links ocean climate and ecosystem change. *Geophysical*
674 *Research Letters* **35**, L08607.
675 Dortch Q., Postel J.R. (1989). Biochemical indicators of N utilization by phytoplankton during
676 upwelling off the Washington coast. *Limnology and Oceanography* **34**, 758-773.
677 Du X., Peterson W.T. (2014). Seasonal cycle of phytoplankton community composition in the
678 coastal upwelling system off central Oregon in 2009. *Estuaries and Coasts* **37**, 299-311.
679 Du X., Peterson W., O'Higgins L. (2015). Interannual variations in phytoplankton community
680 structure in the northern California Current during the upwelling seasons of 2001 – 2010.
681 *Marine Ecology Progress Series* **519**, 75-87.

682 Espinasse B., Hunt B.P., Batten S.D., Pakhomov E.A. (2020). Defining isoscapes in the
683 Northeast Pacific as an index of ocean productivity. *Global Ecology and Biogeography*
684 **29**, 246-261.
685 Frank, K.T., Fisher J.A.D., Leggett W.C. (2015). The spatio-temproal dynamics of trophic
686 control in large marine ecosystems. In: Hanley, T.C. and K.J. La Pierre (Eds.) Trophic
687 Ecology (pp. 31-54). Cambridge University press, Cambridge, United Kingdom.
688 Fox J., Weisberg S. 2019. An R companion to applied regression, Third edition. Sage, Thousand
689 Oaks, CA.
690 Fry B. (2006). Using Stable Isotope Tracers In: Stable Isotope Ecology (pp. 40-75). Springer,
691 New York, New York.
692 Germain L.R., Koch P.L., Harvey J., McCarthy M.D. (2013). Nitrogen isotope fractionation in
693 amino acids from harbor seals: implicatios for compound-specific trophic position
694 calculations. *Marine Ecology Progress Series* **482**, 265-277.
695 Graham B.S., Koch P.L., Newsome S.D., McMahon K.W., Aurioles, D. (2010). Using isoscapes
696 to trace the movements and foraging behavior of top predators in the oceanic ecosystem
697 In: J.B. West, G.J. Bowen, T.E. Dawson, K.P. Tu (Eds.), Isoscapes (pp. 299-318). Spring,
698 Berlin.
699 Granger J., Prokopenko M.G., Sigman D.M., Mordy C.W., Morse Z.M., Morales L.V.,
700 Sambrotto R.N., Plessen B. (2011). Coupled nitrification-denitrification in sediment of
701 the eastern Bering Sea shelf leads to ^{15}N enrichment of the fixed N in shelf waters.
702 *Journal of Geophysical Research* **116**, C11006.
703 Gregg W.W., Conkright M.E., Ginoux P., O'Reilly J.E., Casey N.W. (2003). Ocean primary
704 production and climate: Global decadal changes. *Geophysical Research Letters* **30,** 1809.
705 Hinga K.R., Arthur M.A., Pilson M.E.Q., Whitaker D. (1994). Carbon isotope fractionation by
706 marine phytoplankton in culture: The effects of CO_2 concentration, pH, temperature, and
707 species. *Global Biogeochemical Cycles* **8**, 91-102.
708 Hobson K.A., Clark R.G. (1992). Assessing avian diets using stable isotopes I: turnover of ^{13}C in
709 tissues. *The Condor* **94**, 181-188.
710 Hobson K.A., Schell D.M., Renouf D., Noseworthy E. (1996). Stable carbon and nitrogen
711 isotopic fractionation between diet and tissues of captive seals: implications for dietary

reconstruction involving marine mammals. *Canadian Journal of Fisheries and Aquatic Sciences* **53**, 528-533.

Hoegh-Guldberg O., Bruno J.F. (2010). The impact of climate change on the world's marine ecosystems. *Science* **328**, 1523-1528.

Howe E.R., Simenstad C.A. (2015). Using stable isotopes to discern mechanisms of connectivity in estuarine detritus-based food webs. *Marine Ecology Progress Series* **518**: 13-29.

Jennings S., Brander K. (2010). Predicting the effects of climate change on marine communities and the consequences for fisheries. *Journal of Marine Systems* **79**, 418-426.

Jorgenson J.C, Ward E.J., Scheuerell M.D., Zabel R.W. (2016). Assessing spatial covariance among time series of abundance. *Ecology and Evolution* **6**, 2472-2485.

Jungbluth M.J., Selph K.E., Lenz P.H., Goetze E. (2017). Species-specific grazing and significant trophic impacts by two species of copepod nauplii, *Parvocalanus crassirostris* and *Bestiolina similis. Marine Ecology Progress Series* **572**, 57-76.

Kudela R.M., Banas N.S., Barth J.A., Frame E.R., Jay D.A., Largier J.L., Lessard E.J., Peterson T.D., Vander Woude A.J. (2008). Controls and mechanisms of plankton productivity in coastal upwelling waters of the northern California Current system. *Oceanography* **46**, 46-59.

Kudela R., Peterson T.D. (2009). Influence of a buoyant river plume n phytoplankton nutrient dynamics: what controls standing stocks and productivity? *Journal of Geophysical Research* **114**, C00B11.

Kwiatkowski L., Bopp L., Aumont O., Ciais P., Cox P.M., Laufkötter C., Li Y., Séférian R. (2017). Emergent constraints on projections of declining primary production in the tropical oceans. *Nature Climate Change* 7, 355-358.

Lance M.M., Wan-Ying C., Jeffries S.J., Pearson S.F., Acevedo-Gutiérrez A. (2012). Harbor seal diet in northern Puget Sound: implications for the recovery of depressed fish stocks. *Marine Ecology Progress Series* **464**, 257-271.

Lehmann M.F., Sigman D.M., McCorkle D.C., Brunelle B.G., Hoffmann S., Kienast M., Cane G., Clement J. (2005). Origin of the deep Bering Sea nitrate deficit: constraints from the nitrogen and oxygen isotopic composition of water column nitrate and benthic nitrate fluxes. *Global Biogeochemical Cycles* **19**, GB4005.

742 Litzow M.A., Hunsicker M.E., Bond N.A., Burke B.J., Cunningham C.J., Gosselin J.L., Norton
743 E.L., Ward E.J., Zador S.G. (2020). The changing physical and ecological meanings of
744 North Pacific Ocean climate indices. *PNAS* **117**, 7665-7671.
745 Lorrain A., Pethybridge H., Cassar N., Receveur A., Allain V., Bodin N., Bopp L., Choy C.A.,
746 Duffy L., Fry B., Goñi N., Graham B.S., Hobday A.J., Logan J.M., Ménard F., Menkes
747 C.E., Olson R.J., Pagendam D.E., Point D., Revill A.T., Somes C.J., Young J.W. (2019).
748 Trends in tuna carbon isotopes suggest global changes in pelagic phytoplankton
749 communities. *Global Change Biology* **26**, 458-470.
750 Lowry L.F., Frost K.J., Ver Hoep J.M., Delong R.A. (2001). Movements of satellite-tagged
751 subadult and adult harbor seals in Prince William Sound, Alaska. *Marine Mammal*
752 *Science* **17**, 835-861.
753 Mantua N.J., Hare S.R., Zhang Y., Wallace J.M., Francis R.C. (1997). A Pacific interdecadal
754 climate oscillation with impacts on salmon production. *Bulletin of the American*
755 *Meteorological Society* **78**, 1069-1079.
756 Mantua N.J., Hare S.R. (2002). The Pacific Decadal Oscillation. *Journal of Oceanography* **58**,
757 35-44.
758 Marinov I., Doney S.C., Lima I.D. (2010). Response of ocean phytoplankton community
759 structure to climate change over the 21st century: partitioning the effects of nutrients, t
760 emperature and light. *Biogeosciences* **7**, 3941-3959.
761 McCann K.S., Rasmussen, Umbanhowar J. (2005). The dynamic of spatially coupled food webs.
762 *Ecology Letters* **8**, 513-523.
763 McClelland J.W., Montoya J.W. (2002). Trophic relationships and the nitrogen isotopic
764 composition of amino acids in plankton. *Ecology* **83**, 2173-2180.
765 McMahon K.W., McCarthy M.D., Sherwood O.A., Larsen T., Guilderson T.P. (2015).
766 Millennial-scale plankton regime shifts in the subtropical North Pacific Ocean. *Science*
767 **350**, 1530-1533.
768 McMahon K.W., Michelson C.I., Hart T., McCarthy M.D., Patterson W.P., Polito M.J. (2019).
769 Divergent trophic responses of sympatric penguin species to historic anthropogenic
770 exploitation and recent climate change. *PNAS* **116**, 25721-25727.

771 Meunier C.L., Boersma M., Wiltshire K.H., Malzahn A.M. (2015). Zooplankton eat what they
772 need: copepod selective feeding and potential consequences for marine systems. *Oikos*
773 **125**, 50-58.
774 Misarti N., Finney B., Maschner H., Wooller M.J. (2009). Changes in the northeast Pacific
775 marine ecosystems over the last 4500 years: evidence from stable isotope analysis of
776 bone collagen from archaeological middens. *The Holocene* **19**, 1139-1151.
777 Mohamedali T, Roberts M, Sackmann BS, Kolosseus A (2011) Puget Sound dissolved oxygen
778 model: nutrient load summary for 1999–2008. Publication no. 11-03-057, Washington
779 State Department of Ecology, Olympia, Washington.
780 Moore J.K., Fu W., Primeau F., Britten G.L., Lindsay K., Long M., Dney S.C., Mahowald N.,
781 Hoffman F., Randerson J.T. (2018). Sustained climate warming drives declining marine
782 biological productivity. *Science* **359**, 1139-1143.
783 Morales L.V., Granger J., Chang B.X., Prokopenko M.G., Plessen B., Gradinger R., Sigman
784 D.M. (2014). Elevated $^{15}N/^{14}N$ in particulate organic matter, zooplankton, and diatom
785 frustule-bound nitrogen in the ice-covered water column of the Bering Sea eastern shelf.
786 *Deep Sea Research Part II: Topical Studies in Oceanography* **109**, 100-111.
787 Munch S.B., Giron-Nava A., Sugihara G. (2018). Nonlinear dynamics and noise in fisheries
788 recruitment: A global meta-analysis. *Fish and Fisheries* **19**, 964-973.
789 Naimi B., Hamm N.A.S., Groen T.A., Skidmore A.K., Toxopeus A.G. (2014). Where is
790 positional uncertainty a problem for species distribution modelling? *Ecography* **37**, 191-
791 203.
792 Narwani A., Mazumder A. (2012). Bottom-up effects of species diversity on the functioning and
793 stability of food webs. *Journal of Animal Ecology* **81**, 701-713.
794 Nielsen J.M., Popp B.N., Winder M. (2015). Meta-analysis of amino acid stable nitrogen isotope
795 ratios for estimating trophic position in marine organisms. *Oecologia* **178**, 631-642.
796 Ohkouchi N., Chikaraishi Y., Close H.G., Fry B., Larsen T., Madigan D.J., McCarthy M.D.,
797 McMahon K.W., Nagata T., Naito Y.I., Ogawa N.O., Popp B.N., Steffan S., Takano Y.,
798 Tayasu I., Wyatt A.S.J., Yamaguchi Y.T., Yokoyama Y. (2017). Advances in the
799 application of amino acid nitrogen isotopic analysis in ecological and biogeochemical
800 studies. *Organic Geochemistry* **113**, 150-174.

Ohlberger J., Scheuerell M.D., Schindler D.E. (2016). Population coherence and environmental impacts across spatial scales: a case study of Chinook salmon. *Ecosphere* **7**, e01333.

PSEMP Marine Waters Workgroup. (2019). Puget Sound marine waters: 2018 overview. S. K. Moore, R. Wold, B. Curry, K. Stark, J. Bos, P. Williams, N. Hamel, J. Apple, S. Kim, A. Brown, C. Krembs, and J. Newton (Eds.)

Puerta P., Ciannelli L., Rykaczewski R.R., Opiekun M., Litzow M.A. (2019). Do Gulf of Alaska fish crustacean populations show synchronous non-stationary responses to climate? *Progress in Oceanography* **175**, 161-170.

Quay P.D., Tilbrook B., Wong C.S. (1992). Oceanic uptake of fossil-fuel CO_2-^{13}C evidence. *Science* **256**, 74-79.

R Core Team (2019). R: A language and environment for statistical computing. R Foundation for Statistical Computing, Vienna, Austria. https://www.R-project.org/.

Rooney N., McCann K., Gellner G., Moore J.C. (2006). Structural asymmetry and the stability of diverse food webs. *Nature* **442**, 265-269.

Sherwood O.A., Guilderson T.P., Batista F.C., Schiff J.T., McCarthy M.D. (2014). Increasing subtropical North Pacific Ocean nitrogen fixation since the Little Ice Age. *Nature* **505**, 78-81.

Sherwood O.A., Lehmann M.F., Schubert C.J., Scott D.B., McCarthy M.D. (2011). Nutrient regime shift in the western North Atlantic indicated by compound-specific $\delta^{15}N$ of deep-sea gorgonian corals. *PNAS* **108**, 1011-1015.

Smith S.L., Henrichs S.M., Rho T. (2002). Stable C and N isotopic composition of sinking particles and zooplankton over the southeastern Bering Sea shelf. *Deep-Sea Research II* **49**, 6031-6050.

Stabeno P.J., Bond N.A., Salo S.A. (2007). On the recent warming of the southeastern Bering Sea shelf. *Deep Sea Research Part II: Topical Studies in Oceanography* **54**, 2599-2618.

Stachura M.M., Essington T.E., Mantua N.J., Hollowed A.B., Haltuch M.A., Spencer P.D., Branch T.A., Doyle M.J. (2014). Linking Northeast Pacific recruitment synchrony to environmental variability. *Fisheries Oceanogrpahy* **23**, 389-408.

Stan Development Team (2019). RStan: the R interface to Stan. R package version 2.19.2. http://mc-stan.org/.

831 Strom S.L., Brady Olson M., Macri E.L., Mordy C.W. (2006). Cross-shelf gradients in
832 phytoplankton community structure, nutrient utilization, and growth rate in the coastal Gulf
833 of Alaska. *Marine Ecology Progress Series* **328**, 75-92.
834 Tagliabu A., Bopp L. (2008). Towards understanding global variability in ocean carbon-13.
835 *Global Biogeochemical Cycles* **22**, GB1025.
836 van Klinken G.J. (1999). Bone collagen quality indicators for palaeodietary and radiocarbon
837 measurements. *Journal of Archaeological Science* **26**, 687-695.
838 Vecchi G.A., Wittenberg A.T. (2010). El Niño and our future climate: where do we stand?
839 *WIREs Climate Change* **1**, 260-270.
840 Vehtari A., Gelman A., Gabry J. (2017). Practical Bayesian model evaluation using leave-one-
841 out cross-validation and WAIC. *Statistics and Computing* **27**, 1413-1432.
842 Vokhshoori N.L., McCarthy M.D. (2014). Compound-specific δ^{15}N amino acid measurement in
843 littoral mussels in the California upwelling ecosystem: A new approach to generating
844 baseline δ^{15}N isoscapes for coastal ecosystems. *PLoS ONE* **9**, e98087.
845 Waite J.N., Mueter F.J. (2013). Spatial and temporal variability of chlorophyll-*a* concentrations
846 in the coastal Gulf of Alaska, 1998-2011, using cloud-free reconstructions of SeaWiFS and
847 MODIS-Aqua data. *Progress in Oceanogrpahy* **116**, 179-192.
848 Ware D.M., Thomson R.E. (2005). Bottom-up ecosystem trophic dynamics determine fish
849 production in the Northeast Pacific. *Science* **308**, 1280-1284.
850 Whitney N.M., Johnson B.J., Dostie P.T., Luzier K., Wanamaker A.D. (2019). Paired bulk
851 organic and individual amino acid δ^{15}N analyses of bivalve shell peristracum: A
852 paleoceanographic proxy for water source variability and nitrogen cycling processes.
853 *Geochimica et Cosmochimica Acta* **254**, 67-85.
854 Whitney F.A, Welch D.W. (2002). Impact of the 1997-1998 El Niño and La Niña on nutrient
855 supply in the Gulf of Alaska. *Progress in Oceanography* **54**, 405-421.
856 Williams B., Risk M., Stone R., Sinclair D., Ghaleb B. (2007). Oceanographic changes in the
857 North Pacific Ocean over the past century recorded in deep-water gorgonian corals.
858 *Marine Ecology Progress Series* **335**, 85-94.
859 Wu J., Clavert S.E., Wong C.S. (1997). Nitrogen isotope variations in the subarctic northeast
860 Pacific: relationships to nitrate utilization and trophic structure. *Deep Sea Research Part*
861 *1: Oceanographic Research Papers* **44**, 287-314.

862 Zuur A.F., Tuck I.D., Bailey N. (2003). Dynamic factor analyses to estimate common trends in
863 fisheries time series. *Canadian Journal of Fisheries and Aquatic Science* **60**, 542-552.

A. Discharge introduces terrestrial C and anthropogenic N (wastewater treatment, agricultural runoff), and limiting nutrients such as Fe to marine food webs

NO_3^-, NH_4^+, urea, CO_2, Fe, Si, P

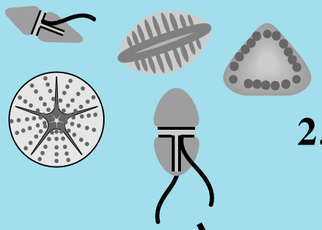

1. Available C and N (anthropogenic, terrestrial, regenerated, deep ocean) are assimilated into phytoplankton

2. Phytoplankton express $\delta^{15}N$ and $\delta^{13}C$ values based on community composition, available nutrients, and growth rates

D. Changes in sea surface temperature, light limitation, and nutrient availability impact community composition of phytoplankton

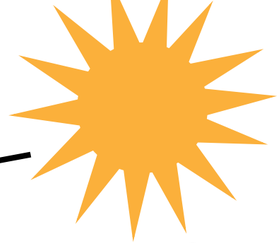

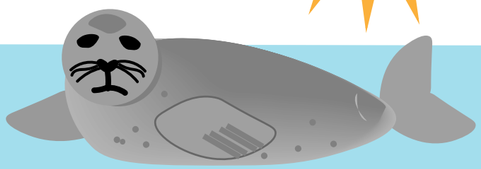

3. Phytoplankton $\delta^{15}N$ and $\delta^{13}C$ values are conserved as they are transfered through the foodweb to top predators, representing a signature of food web-assimilated production and nitrogen

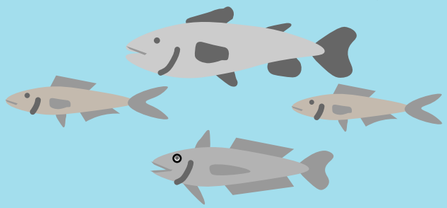

B. Upwelling carries deep ocean nitrate ($\delta^{15}N$ ~5‰) to the euphotic zone where it mixes with regenerated sourc-

NO_3^-

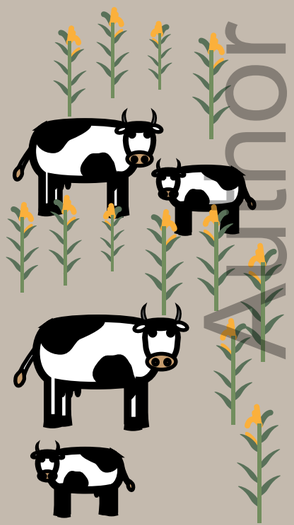

Higher $\delta^{13}C$ values (More productive)

C. $\delta^{13}C$ exhibits a nearshore verse offshore gradient

Lower $\delta^{13}C$ values (Less productive)